Published in final edited form as:
Biochem Biophys Res Commun. 2011 April 22; 407(4): 650–655. doi:10.1016/j.bbrc.2011.03.062.

Long helical filaments are not seen encircling cells in electron cryotomograms of rod-shaped bacteria

Matthew T. Swulius[‡,a], **Songye Chen**[‡,a], **H. Jane Ding**[a], **Zhuo Li**[c], **Ariane Briegel**[a], **Martin Pilhofer**[a,b], **Elitza I. Tocheva**[a], **Suzanne R. Lybarger**[d], **Tanya L. Johnson**[d], **Maria Sandkvist**[d], and **Grant J. Jensen**[a,b,*]

[a]Division of Biology, California Institute of Technology, 1200 E California Blvd, Pasadena, CA 91125

[b]Howard Hughes Medical Institute, California Institute of Technology, 1200 E California Blvd, Pasadena, CA 91125

[c]EM Core Facility, City of Hope, 1500 E Duarte Rd., Duarte, CA 91010

[d]Department of Microbiology and Immunology, University of Michigan Medical School, Ann Arbor, MI 48109

Abstract

How rod-shaped bacteria form and maintain their shape is an important question in bacterial cell biology. Results from fluorescent light microscopy have led many to believe that the actin homolog MreB and a number of other proteins form long helical filaments along the inner membrane of the cell. Here we show using electron cryotomography of six different rod-shaped bacterial species, at macromolecular resolution, that no long (>80 nm) helical filaments exist near or along either surface of the inner membrane. We also use correlated cryo-fluorescent light microscopy (cryo-fLM) and electron cryo-tomography (ECT) to identify cytoplasmic bundles of MreB, showing that MreB filaments are detectable by ECT. In light of these results, the structure and function of MreB must be reconsidered: instead of acting as a large, rigid scaffold that localizes cell-wall synthetic machinery, moving MreB complexes may apply tension to growing peptidoglycan strands to ensure their orderly, linear insertion.

Keywords

MreB; electron cryo-tomography; helical filament; rod-shaped; bacterial shape

Introduction

Many papers have reported evidence of and/or discussed models involving long helical protein filaments surrounding the cytoplasm of rod-shaped bacteria. The first protein reported to form such a helix was MreB. It is known to play a role in the generation and maintenance of rod shape [1,2,3,4,5,6,7] and has also been argued to function in

*To whom correspondence should be addressed: jensen@caltech.edu.
‡These authors contributed equally to this work.

chromosome segregation [8,9,10]. Using fluorescent light microscopy (fLM), MreB was described in *Bacillus subtilis* as localizing in elongated helical patterns encircling cells, just inside the inner membrane [5]. Subsequently, this same pattern was reported for MreB in *Escherichia coli* [6], *Caulobacter crescentus* [3], *Vibrio cholerae* [7] and *Vibrio parahaemolyticus* [1]. Despite sharing weak sequence similarity, X-ray crystallography revealed that MreB and actin are structural homologs [11]. *In vitro*, MreB forms polymers, further supporting the notion that it could form a long helical cytoskeleton [11,12]. In most rod-shaped bacteria, MreB is essential, as in-frame deletions of MreB can only be produced by complementing expression from an inducible promoter. When the inducer is removed, MreB concentrations fall and cells lose their rod shape, eventually lysing [3,4,5,13,14]. Additionally, cells treated with the small molecule A22, which inhibits MreB polymerization, also gradually lose their rod-shape and become spherical [8], a process that is reversible upon removal of the drug. Based on these results and others, it has been widely hypothesized that MreB filaments form long tracks that position cell wall synthetic machinery in such a way that rod-shaped cells result [15,16,17].

Concurrently, electron cryotomography (ECT) has emerged as a powerful new method for visualizing the ultrastructure of small cells in a near-native, "frozenhydrated" state to "macromolecular" (4–6 nm) resolution. Cell cultures are spread into thin films across EM grids, plunged into liquid ethane, and imaged through a range of different angles in an electron cryomicroscope [18]. Three-dimensional reconstructions (tomograms) of cells are then calculated from the images. In just the past few years, cryotomography has revealed the location and structure of numerous cytoskeletal filaments within bacterial cells, including the actin homologs MamK and ParM [19,20,21,22,23,24].

Materials and Methods

Sample preparation and Electron Cryo-Tomography

Cell cultures were grown in standard media and harvested during log-phase growth. For A22 treatment of *Caulobacter* cells, 10 μg/ml of A22 was added to exponentially growing liquid cultures and allowed to incubate for 2 hrs before plunge-freezing. To freeze, 4 μl of cells were pipetted onto a freshly glow-discharged Quantifoil EM grid (R2/2) and plunge-frozen in liquid ethane using an FEI Vitrobot. 10-nm colloidal gold markers were added to the cells prior to freezing for use as fiducial markers during reconstruction. Samples were stored in liquid nitrogen and maintained frozen throughout transfer into and imaging in an FEI G2 Polara transmission electron microscope operating at 300 keV. Energy-filtered 'tilt-series' of images of individual cells were collected automatically from approximately −63° to +63° at 1° intervals using Leginon [25] on a 4k × 4k lens-coupled Gatan UltraCAM. The energy slit-width was 20 eV, the defocus was ~12 μm, the total dose for each tilt-series was ~150–180 $e^{-}/Å^{2}$, and the magnification was set such that each CCD pixel corresponded to between 0.67 and 0.95 nm at the specimen level.

Image processing and Computational Search Methods

Images were binned two-fold before tilt-series were reconstructed using the IMOD package (http://bio3d.colorado.edu/imod/). Segmentation and 3-D visualization were carried out manually using Amira (Mercury Computer Systems). To calculate density profiles near to and including the inner membrane, the cytoplasmic membrane was first segmented manually to generate a triangle-mesh surface. Density values were then sampled and averaged along normals to each triangle using Amira modules developed 'in-house.' Shells up to 16 nm into the cell and as far as 10 nm into the periplasmic space were searched for filaments using shell thicknesses of 2, 4, 6, 8 and 10 nm.

A line-segment-based search algorithm was used in the same regions. The algorithm uses correlations of three dimensional orientation fields to search for thin densities within the tomogram [26]. Because the membrane has high contrast, this method cannot detect filaments in contact with the membrane.

Correlated Cryo-fLM/ECT

V. cholerae cells expressing GFP-MreB from a pMMb67 plasmid were grown in M9 minimal media at 37°C to an OD^{600} of 0.3. 10 μm IPTG was then added to induce expression and the cells were incubated for 90 additional minutes. FM4-64 was added to the media at 5 μg/ml along with 10-nm fiducial gold markers 5 min prior to plunge-freezing on copper EM finder-grids. Plunge-frozen grids were then loaded into a cryo-fLM stage (FEI) mounted on a Nikon 90Ti inverted microscope and imaged using a 60× ELWD air objective.

After imaging cells in the cryo-fLM, grids were transferred (never exceeding −150°C) into the cryo-EM. Tabs on the finder-grid were used to relocate the cells imaged by the fLM. Tilt-series from −65 to +65 were collected at 1° increments and tomograms were reconstructed.

To overlay the fluorescent signals on the tomograms, the FM4-64 and GFP signals were thresholded to best match the known shape of *V. cholerae* cells and best reveal the subcellular localization, respectively. Boundaries of the included pixels were then rescaled exactly to match the much higher magnification of the EM data, smoothed, and overlaid onto tomographic slices.

Simulated Filaments in Tomograms

For the positive control cell in Fig. 1D–F, 4-nm simulated filaments were placed inside the experimental tomogram at positions manually segmented on the membrane (#'s 1–7) or 1, 2 or 3 pixels embedded into the membrane (#'s 8–10, respectively). The voxel intensities of the simulated filaments were chosen randomly to match the real FtsZ filaments in the same tomogram. The effect of the missing-wedge on simulated filaments was replicated by replacing the missing-wedge of the modified tomogram in 3-D reciprocal space with the values from the original tomogram.

Results

To investigate whether any proteins such as MreB form long helical filaments around rod shaped bacteria, we collected tomograms from six cell types and searched for filaments along or near the inner membrane. We chose *C. crescentus, B. subtilis, E. coli and V. cholerae*, four classic model organisms where MreB has been reported to form long helices, as well as *Borrelia burgdorferi* and *Acetonema longum*, two extraordinarily slim species that therefore yield the clearest cryotomograms.

No long helical filaments were seen (Figs. 1 and 2). At least two factors could make this type of filament more difficult to recognize than others, however. First, the density of proteins and lipids are approximately the same, so a filament lying directly on the membrane would appear as just a ridge, and if the filament were embedded within the membrane, it would be obscured by contrast-matching. Second, because our most-used visualization tool presents 2-D slices of 3-D volumes, rapidly curving helices could be harder to notice because no single slice would contain a large continuous segment. In addition, because of physical constraints, images tilted past ~65° are not generally included, generating a "missing wedge/pyramid" of data in reciprocal space which obscures filaments lying in the plane of the sample perpendicular to the tilt axis. This effect would not hide helical

filaments, however, since curved pathways exhibit a range of orientations with respect to the electron beam.

To overcome these obstacles and test whether long helical filaments could have escaped visual detection, we searched for filaments near the membrane using two computational methods. First, densities within shells surrounding and sometimes including the inner membrane were projected onto the membrane surface. Such projections reveal filaments even if they are immediately adjacent to the membrane and even if they are highly curved. Second, similar shells were searched for filamentous densities using a line segment-based detection algorithm. Again, no long helical filaments were detected near or along the inner membrane of any of the six species tested (Figs. 1 & 2). While some short streaks can be seen in the averaged density projections near the membrane, we do not think they are attributable to MreB since A22-treated cells yield similar projections (Fig. 2).

As a positive control, the same search methods were applied to a predivisional *C. crescentus* cell possessing several FtsZ filaments. FtsZ filaments can be recognized as either curved or straight, short (~100 nm), 4-nm diameter filaments positioned ~16 nm away from the membrane near the midplane of dividing cells [23]. The filaments were visible by eye and were detected by both algorithms (filaments labeled "a" – "e" in Fig. 1D–F), including one filament ("f") that was unusually close (~6.5 nm center-to-center) to the membrane (distances in tomograms are best measured from density peak to density peak). To explore how helical filaments of different length, pitch, and proximity to the membrane would appear, additional filaments with similar diameters, densities and noise characteristics were simulated within the cell (filaments labeled "1" - "10" in Fig. 1D–F). This was achieved by simply i) setting the densities of selected lines of adjacent voxels to values randomly chosen from within the native filaments and ii) re-imposing the missing wedge in reciprocal space. Simulated filaments #'s 1–7 were positioned immediately adjacent to the membrane (4.5 nm center-to-center), estimating that the membrane is 5-nm thick and the diameter of MreB is 4 nm. Simulated filaments longer than 80 nm were readily detected by eye (using standard visualization methods) as dark bumps on the membrane surface that "ran" up and down the membrane as different tomographic slices were displayed in rapid succession (see Movies S1 and S2). These were also readily detected in projections of the density onto the inner membrane, regardless of the pitch of the helix (Fig. 1E). The filament less than 80 nm in length ("1) was difficult to discern against the noisy background of other densities, however, and filaments “embedded” within the density of the membrane (#'s 8–10) were also undetectable as expected.

To verify that the resolution of our tomograms was sufficient to visualize MreB filaments were they present, we imaged *V. cholerae* cells overexpressing MreB. Large bundles of filaments are seen in the cytoplasm of these cells, which we confirmed to be MreB through correlated cryo-fLM/ECT. To do this, cells expressing GFP-MreB were stained with the membrane dye FM4-64, plunge-frozen on an EM finder-grid and imaged in a "cryo-" fLM (an fLM equipped with a cryo-stage [27]). The grid was then transferred into the EM and the same cells were imaged by ECT. In 8 out of 8 cells imaged where a subcellular fluorescent focus was seen, its location matched well the position of the cytoplasmic bundle (Figs. 3 and S1). Even within these cells overexpressing GFP-MreB there were no long helical filaments detected along the inner membrane of the cell. Moreover, in similar cells without the GFP tag, cytoplasmic MreB filaments were clearly still visible (Fig. 3B). Together, the real and simulated filaments prove that the resolution of the tomograms and the sensitivity of the search methods were sufficient to reveal long helices had they been present either on or outside the membrane.

Discussion

We conclude that there are no long (>80 nm) helical filaments (MreB or otherwise) encircling these bacterial cells on either side of the inner membrane. But how can this result be reconciled with the light microscopy images suggesting long helices? While we think it unlikely, there remains the possibility that either the fLM or ECT results are artifacts of the sample preparation. It is possible, for instance, that MreB and other proteins are induced to form long helices encircling the cell by the conditions used for fLM (i.e. juxtaposition between an agarose pad and a coverslip), or that the long helix-like patterns seen by fLM form simply because the diffusion-accessible space within an immobilized bacterial cell is made helical by a twisted nucleoid [28], concentrating unpolymerized proteins. Likewise, in the cryotomography experiments it is conceivable that the surface tension experienced by the cell during the time between blotting and plunge-freezing causes long helical filaments to depolymerize. This explanation seems unlikely, however, since one would expect exceptions, and except for spirochetal flagella, we have never seen long helical filaments next to the membrane in any of our now ~6000 cryotomograms of individual bacteria or parts thereof from 18 different rod-shaped species.

Instead, since MreB monomers are known to move across the cell in linear, approximately circumferential trajectories [29], we think it more likely that the streaks seen by fLM are caused by small complexes moving during long exposures. In this model, existing peptidoglycan (PG) strands of the cell wall, and not long MreB helices, would be the scaffold that directs further growth [30]. We speculate that the role of moving MreB/cell-wall-synthetic-machinery complexes is to apply tension to nascient PG strands, elongating and straightening them as they are crosslinked to adjacent strands in the existing cell wall. This idea is attractive because something must prevent growing PG strands from simply folding back onto themselves in a ball. We emphasize, however, that our results do not exclude the possibility that short (<80 nm) MreB filaments form. MreB polymerization may in fact be the force that drives locomotion, for instance, and short MreB filaments may bridge across existing PG strands, stiffening cells [31].

Supplementary Material

Refer to Web version on PubMed Central for supplementary material.

Abbreviations

ECT	Electron Cryo-Tomography
fLM	Fluorescent Light Microscopy

Acknowledgments

We thank Drs. Jian Shi and Alasdair McDowall for support of the EM instrumentation. This work was supported by NIH grant R01 AI067548 to GJJ and the Gordon and Betty Moore Center for Integrative Study of Cell Regulation. Work done by MS was supported by NIH grant RO1 AI049294.

References

1. Chiu SW, Chen SY, Wong HC. Dynamic localization of MreB in Vibrio parahaemolyticus and in the ectopic host bacterium *Escherichia coli*. Appl Environ Microbiol. 2008; 74:6739–6745. [PubMed: 18791022]
2. Defeu Soufo HJ, Graumann PL. Dynamic movement of actin-like proteins within bacterial cells. EMBO Rep. 2004; 5:789–794. [PubMed: 15272301]

3. Figge RM, Divakaruni AV, Gober JW. MreB, the cell shape-determining bacterial actin homologue, co-ordinates cell wall morphogenesis in *Caulobacter crescentus*. Mol Microbiol. 2004; 51:1321–1332. [PubMed: 14982627]
4. Formstone A, Errington J. A magnesium-dependent mreB null mutant: implications for the role of mreB in *Bacillus subtilis*. Mol Microbiol. 2005; 55:1646–1657. [PubMed: 15752190]
5. Jones LJ, Carballido-Lopez R, Errington J. Control of cell shape in bacteria: helical, actin-like filaments in *Bacillus subtilis*. Cell. 2001; 104:913–922. [PubMed: 11290328]
6. Shih YL, Le T, Rothfield L. Division site selection in *Escherichia coli* involves dynamic redistribution of Min proteins within coiled structures that extend between the two cell poles. Proc Natl Acad Sci U S A. 2003; 100:7865–7870. [PubMed: 12766229]
7. Srivastava P, Demarre G, Karpova TS, McNally J, Chattoraj DK. Changes in nucleoid morphology and origin localization upon inhibition or alteration of the actin homolog, MreB, of *Vibrio cholerae*. J Bacteriol. 2007; 189:7450–7463. [PubMed: 17704222]
8. Gitai Z, Dye NA, Reisenauer A, Wachi M, Shapiro L. MreB actin-mediated segregation of a specific region of a bacterial chromosome. Cell. 2005; 120:329–341. [PubMed: 15707892]
9. Kruse T, Moller-Jensen J, Lobner-Olesen A, Gerdes K. Dysfunctional MreB inhibits chromosome segregation in *Escherichia coli*. EMBO J. 2003; 22:5283–5292. [PubMed: 14517265]
10. Shebelut CW, Jensen RB, Gitai Z. Growth conditions regulate the requirements for Caulobacter chromosome segregation. J Bacteriol. 2009; 191:1097–1100. [PubMed: 19028887]
11. van den Ent F, Amos LA, Lowe J. Prokaryotic origin of the actin cytoskeleton. Nature. 2001; 413:39–44. [PubMed: 11544518]
12. Popp D, Narita A, Maeda K, Fujisawa T, Ghoshdastider U, Iwasa M, Maeda Y, Robinson RC. Filament structure, organization, and dynamics in MreB sheets. J Biol Chem. 2010; 285:15858–15865. [PubMed: 20223832]
13. Kruse T, Bork-Jensen J, Gerdes K. The morphogenetic MreBCD proteins of *Escherichia coli* form an essential membrane-bound complex. Mol Microbiol. 2005; 55:78–89. [PubMed: 15612918]
14. Slovak PM, Wadhams GH, Armitage JP. Localization of MreB in *Rhodobacter sphaeroides* under conditions causing changes in cell shape and membrane structure. J Bacteriol. 2005; 187:54–64. [PubMed: 15601688]
15. Carballido-Lopez R, Formstone A, Li Y, Ehrlich SD, Noirot P, Errington J. Actin homolog MreBH governs cell morphogenesis by localization of the cell wall hydrolase LytE. Dev Cell. 2006; 11:399–409. [PubMed: 16950129]
16. Divakaruni AV, Baida C, White CL, Gober JW. The cell shape proteins MreB and MreC control cell morphogenesis by positioning cell wall synthetic complexes. Mol Microbiol. 2007; 66:174–188. [PubMed: 17880425]
17. Kawai Y, Daniel RA, Errington J. Regulation of cell wall morphogenesis in *Bacillus subtilis* by recruitment of PBP1 to the MreB helix. Mol Microbiol. 2009; 71:1131–1144. [PubMed: 19192185]
18. Tocheva EI, Li Z, Jensen GJ. Electron cryotomography. Cold Spring Harb Perspect Biol. 2010; 2 a003442.
19. Briegel A, Dias DP, Li Z, Jensen RB, Frangakis AS, Jensen GJ. Multiple large filament bundles observed in *Caulobacter crescentus* by electron cryotomography. Mol Microbiol. 2006; 62:5–14. [PubMed: 16987173]
20. Komeili A, Li Z, Newman DK, Jensen GJ. Magnetosomes are cell membrane invaginations organized by the actin-like protein MamK. Science. 2006; 311:242–245. [PubMed: 16373532]
21. Kurner J, Frangakis AS, Baumeister W. Cryo-electron tomography reveals the cytoskeletal structure of *Spiroplasma melliferum*. Science. 2005; 307:436–438. [PubMed: 15662018]
22. Li Z, Trimble MJ, Brun YV, Jensen GJ. The structure of FtsZ filaments in vivo suggests a force-generating role in cell division. EMBO J. 2007; 26:4694–4708. [PubMed: 17948052]
23. Salje J, Zuber B, Lowe J. Electron cryomicroscopy of *E. coli* reveals filament bundles involved in plasmid DNA segregation. Science. 2009; 323:509–512. [PubMed: 19095899]
24. Scheffel A, Gruska M, Faivre D, Linaroudis A, Plitzko JM, Schuler D. An acidic protein aligns magnetosomes along a filamentous structure in magnetotactic bacteria. Nature. 2006; 440:110–114. [PubMed: 16299495]

25. Suloway C, Pulokas J, Fellmann D, Cheng A, Guerra F, Quispe J, Stagg S, Potter CS, Carragher B. Automated molecular microscopy: the new Leginon system. J Struct Biol. 2005; 151:41–60. [PubMed: 15890530]

26. Sandberg K, Brega M. Segmentation of thin structures in electron micrographs using orientation fields. J Struct Biol. 2007; 157:403–415. [PubMed: 17116405]

27. Briegel A, Chen S, Koster AJ, Plitzko JM, Schwartz CL, Jensen GJ. Correlated light and electron cryo-microscopy. Methods Enzymol. 2010; 481:317–341. [PubMed: 20887863]

28. Butan C, Hartnell LM, Fenton AK, Bliss D, Sockett RE, Subramaniam S, Milne JL. Spiral architecture of the nucleoid in *Bdellovibrio bacteriovorus*. J Bacteriol. 2010

29. Kim SY, Gitai Z, Kinkhabwala A, Shapiro L, Moerner WE. Single molecules of the bacterial actin MreB undergo directed treadmilling motion in *Caulobacter crescentus*. Proc Natl Acad Sci U S A. 2006; 103:10929–10934. [PubMed: 16829583]

30. Gan L, Chen S, Jensen GJ. Molecular organization of Gram-negative peptidoglycan. Proc Natl Acad Sci U S A. 2008; 105:18953–18957. [PubMed: 19033194]

31. Wang S, Arellano-Santoyo H, Combs PA, Shaevitz JW. Actin-like cytoskeleton filaments contribute to cell mechanics in bacteria. Proc Natl Acad Sci U S A. 2010; 107:9182–9185. [PubMed: 20439764]

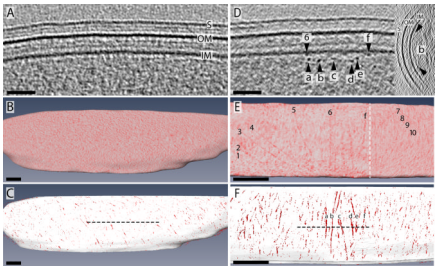

Figure 1. No long filaments are seen encircling rod shaped bacteria

A) 45-nm thick tomographic slice through a *C. crescentus* swarmer cell along the cell envelope. The inner membrane (IM), outer membrane (OM) and surface layer (S) are visible, but there are no filaments near the inner membrane. B) Projections onto the inner membrane of all the density from the periplasmic face of the inner membrane to 13 nm into the cytoplasm. Red represents higher density. C) Line-segment-based search for filaments 21 nm into the cell counted from the center of the inner membrane. Red pixels are those identified as potentially belonging to filaments. The position of the slice shown in A is marked with a dashed line. D) Analogous 45-nm slice, E) density projection, F) and filament search of a predivisional *C. crescentus* "positive control" cell possessing 6 native ("a" – "f") and 10 simulated ("1" – "10") filaments. The insert in D shows a side view including native filament “b”(arrowheads). The simulated filaments of different lengths (#'s 1–4, which are 40, 80, 120, and 180 nm long, respectively) show that filaments 80 nm or longer are clear. Simulated filaments #4–7 exhibit different pitches with respect to the long axis of the cell, but are all equally visible. Filaments #1–7 are immediately adjacent to the membrane, but filaments #8–10 cannot be seen as they range from partially to fully embedded, positioned successively one pixel (1.3 nm) each deeper into the membrane. To the left of the dashed white line in E, the projected shell was optimized to show the filaments next to the membrane, and extended from the cytoplasmic face of the inner membrane to 13 nm into the cytoplasm. To the right, the projection is of the same shell shown in B (including the membrane). Scale bars represent 50 nm for (A & D) and 100 nm for (B, C, E and F).

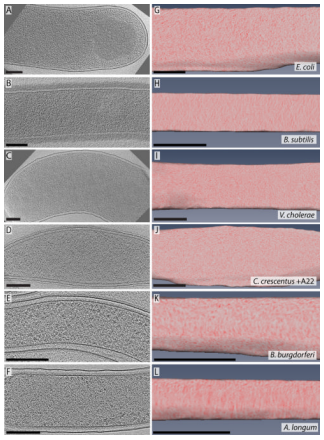

Figure 2. Long helixes are not seen encircling rod shaped bacteria

Shown are tomographic slices (A–F) and density projections onto the inner membrane of all the densities between the periplasmic edge of the inner membrane to 13 nm into the cytoplasm (G–L) of all the cell types where MreB has been reported to form long helical filaments encircling the cell (*E. coli*, *B. subtilis*, *V. cholera*, with *C. crescentus* shown in Fig. 1 of the main text), plus *C. crescentus* treated with A22 (a small molecule known to depolymerize MreB filaments), plus *B. burgdorferi* and *A. longum*, which are especially slender and therefore yield the highest resolution cryotomograms. All scale bars represent 200 nm.

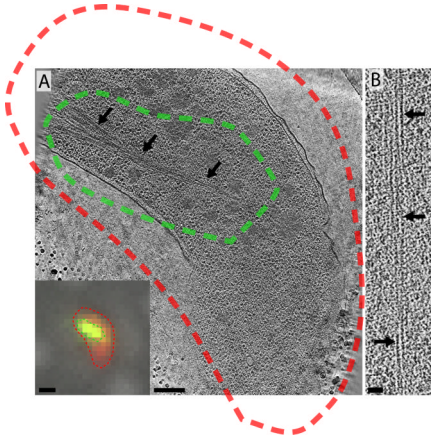

Figure 3. Cytoplasmic MreB filaments are clearly visible in cryotomograms

A) Tomographic slice through a *V. cholerae* cell overexpressing GFP-MreB. The inset shows the image taken by cryo-fLM. Red is the membrane-dye FM4-64 and green is GFP-MreB. Dashed lines (red and green) represent the thresholded boundaries of each signal, respectively. The dashed lines generated from the cryo-fLM image were rescaled to match the much higher magnification of the EM slice and superimposed to show the GFP signal appears in the same location as a large filament bundle running through the cytoplasm (arrows), proving upon repetition that these bundles are composed of MreB. B)15-nm thick tomographic slice though an MreB bundle (not fused to GFP). Arrows point to filaments within the bundle. Scale bars represent 1 μm in the fLM inset of A, 200 nm in the ECT slice of A and 50 nm in B.